

Excited state energies and scattering phase shifts from lattice QCD with the stochastic LapH method

Andrew Hanlon and Jake Fallica
University of Pittsburgh, Carnegie Mellon University

6th Workshop of the APS Topical Group on Hadronic Physics

Baltimore, MD

April 10, 2015

Outline

- project goals:
 - comprehensive survey of QCD stationary states in finite volume
 - hadron scattering phase shifts, decay widths
- preliminary results for 20 channels $I = 1, S = 0$
 - correlator matrices of size 100×100
 - large number of extended single-hadron operators
 - attempt to include all needed 2-hadron operators
- preliminary results for $I = \frac{1}{2}, S = 1, T_{1u}$
- very preliminary results for $I = 0, S = 0, A_{1u}^+$
- $I = 1$ P -wave $\pi\pi$ scattering phase shifts and width of ρ

Extended operators for single hadrons

- quark displacements build up orbital, radial structure

Meson configurations



Baryon configurations



$$\bar{\Phi}_{\alpha\beta}^{AB}(\mathbf{p}, t) = \sum_{\mathbf{x}} e^{i\mathbf{p}\cdot(\mathbf{x} + \frac{1}{2}(\mathbf{d}_\alpha + \mathbf{d}_\beta))} \delta_{ab} \bar{q}_{b\beta}^B(\mathbf{x}, t) q_{a\alpha}^A(\mathbf{x}, t)$$

$$\bar{\Phi}_{\alpha\beta\gamma}^{ABC}(\mathbf{p}, t) = \sum_{\mathbf{x}} e^{i\mathbf{p}\cdot\mathbf{x}} \varepsilon_{abc} \bar{q}_{c\gamma}^C(\mathbf{x}, t) \bar{q}_{b\beta}^B(\mathbf{x}, t) \bar{q}_{a\alpha}^A(\mathbf{x}, t)$$

- group-theory projections onto irreps of lattice symmetry group

$$\bar{M}_l(t) = c_{\alpha\beta}^{(l)*} \bar{\Phi}_{\alpha\beta}^{AB}(t) \quad \bar{B}_l(t) = c_{\alpha\beta\gamma}^{(l)*} \bar{\Phi}_{\alpha\beta\gamma}^{ABC}(t)$$

- definite momentum \mathbf{p} , irreps of little group of \mathbf{p}

Two-hadron operators

- our approach: superposition of products of single-hadron operators of definite momenta

$$C_{\mathbf{p}_a \lambda_a; \mathbf{p}_b \lambda_b}^{I_{3a} I_{3b}} B_{\mathbf{p}_a \Lambda_a \lambda_a i_a}^{I_a I_{3a} S_a} B_{\mathbf{p}_b \Lambda_b \lambda_b i_b}^{I_b I_{3b} S_b}$$

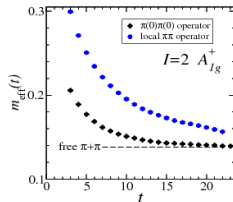
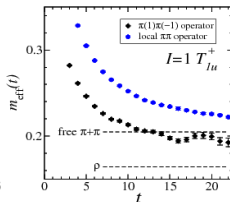
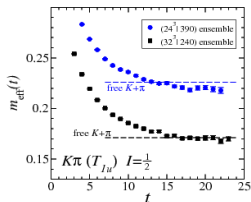
- fixed total momentum $\mathbf{p} = \mathbf{p}_a + \mathbf{p}_b$, fixed $\Lambda_a, i_a, \Lambda_b, i_b$
- group-theory projections onto little group of \mathbf{p} and isospin irreps
- restrict attention to certain classes of momentum directions
 - on axis $\pm \hat{x}, \pm \hat{y}, \pm \hat{z}$
 - planar diagonal $\pm \hat{x} \pm \hat{y}, \pm \hat{x} \pm \hat{z}, \pm \hat{y} \pm \hat{z}$
 - cubic diagonal $\pm \hat{x} \pm \hat{y} \pm \hat{z}$
- efficient creating large numbers of two-hadron operators
- generalizes to three, four, . . . hadron operators

Testing our two-meson operators

- (left) $K\pi$ operator in T_{1u} $I = \frac{1}{2}$ channels
- (center and right) comparison with localized $\pi\pi$ operators

$$(\pi\pi)^{A_{1g}^+}(t) = \sum_{\mathbf{x}} \pi^+(\mathbf{x}, t) \pi^+(\mathbf{x}, t),$$

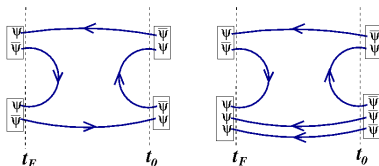
$$(\pi\pi)^{T_{1u}^+}(t) = \sum_{\mathbf{x}, k=1,2,3} \left\{ \pi^+(\mathbf{x}, t) \Delta_k \pi^0(\mathbf{x}, t) - \pi^0(\mathbf{x}, t) \Delta_k \pi^+(\mathbf{x}, t) \right\}$$



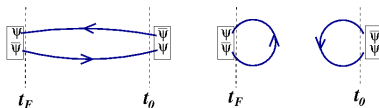
- less contamination from higher states in our $\pi\pi$ operators

Quark line diagrams

- temporal correlations involving our two-hadron operators need
 - slice-to-slice quark lines (from all spatial sites on a time slice to all spatial sites on another time slice)
 - sink-to-sink quark lines



- isoscalar mesons also require sink-to-sink quark lines



- solution: the stochastic LapH method!

Stochastic estimation of quark propagators

- do not need exact inverse of Dirac matrix $K[U]$
- use noise vectors η satisfying $E(\eta_i) = 0$ and $E(\eta_i \eta_j^*) = \delta_{ij}$
- Z_4 noise is used $\{1, i, -1, -i\}$
- solve $K[U]X^{(r)} = \eta^{(r)}$ for each of N_R noise vectors $\eta^{(r)}$, then obtain a Monte Carlo estimate of all elements of K^{-1}

$$K_{ij}^{-1} \approx \frac{1}{N_R} \sum_{r=1}^{N_R} X_i^{(r)} \eta_j^{(r)*}$$

- variance reduction using noise dilution
- dilution introduces projectors

$$P^{(a)} P^{(b)} = \delta^{ab} P^{(a)}, \quad \sum_a P^{(a)} = 1, \quad P^{(a)\dagger} = P^{(a)}$$

- define $\eta^{[a]} = P^{(a)} \eta$, $X^{[a]} = K^{-1} \eta^{[a]}$

to obtain Monte Carlo estimate with drastically reduced variance

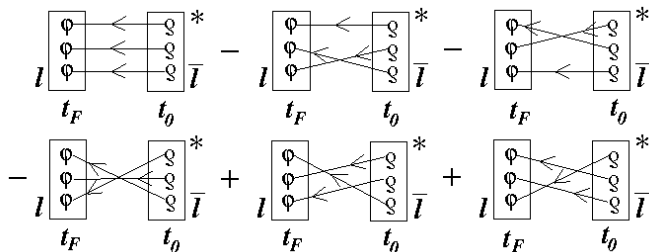
$$K_{ij}^{-1} \approx \frac{1}{N_R} \sum_{r=1}^{N_R} \sum_a X_i^{(r)[a]} \eta_j^{(r)[a]*}$$

Correlators and quark line diagrams

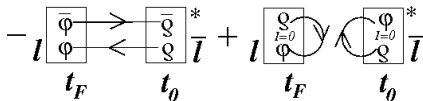
- baryon correlator

$$C_{\bar{l}l} \approx \frac{1}{N_R} \sum_r \sum_{d_A d_B d_C} \mathcal{B}_l^{(r)[d_A d_B d_C]}(\varphi^A, \varphi^B, \varphi^C) \mathcal{B}_{\bar{l}}^{(r)[d_A d_B d_C]}(\varrho^A, \varrho^B, \varrho^C)^*$$

- express diagrammatically

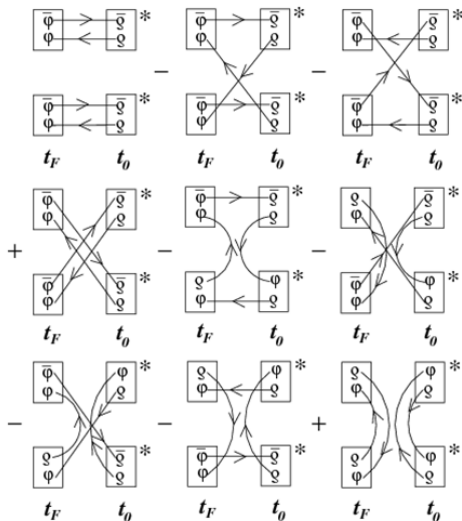


- meson correlator



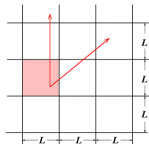
More complicated correlators

- two-meson to two-meson correlators (non isoscalar mesons)



Quantum numbers in toroidal box

- periodic boundary conditions in cubic box
 - not all directions equivalent \Rightarrow using J^{PC} is wrong!!



- label stationary states of QCD in a periodic box using irreps of cubic space group **even in continuum limit**

- zero momentum states: little group O_h

$$A_{1a}, A_{2ga}, E_a, T_{1a}, T_{2a}, G_{1a}, G_{2a}, H_a, \quad a = g, u$$

- on-axis momenta: little group C_{4v}

$$A_1, A_2, B_1, B_2, E, G_1, G_2$$

- planar-diagonal momenta: little group C_{2v}

$$A_1, A_2, B_1, B_2, G_1, G_2$$

- cubic-diagonal momenta: little group C_{3v}

$$A_1, A_2, E, F_1, F_2, G$$

- include G parity in some meson sectors (superscript $+$ or $-$)

Spin content of cubic box irreps

- numbers of occurrences of Λ irreps in J subduced

J	A_1	A_2	E	T_1	T_2
0	1	0	0	0	0
1	0	0	0	1	0
2	0	0	1	0	1
3	0	1	0	1	1
4	1	0	1	1	1
5	0	0	1	2	1
6	1	1	1	1	2
7	0	1	1	2	2

J	G_1	G_2	H	J	G_1	G_2	H
$\frac{1}{2}$	1	0	0	$\frac{9}{2}$	1	0	2
$\frac{3}{2}$	0	0	1	$\frac{11}{2}$	1	1	2
$\frac{5}{2}$	0	1	1	$\frac{13}{2}$	1	2	2
$\frac{7}{2}$	1	1	1	$\frac{15}{2}$	1	1	3

Common hadrons

- irreps of commonly-known hadrons at rest

Hadron	Irrep	Hadron	Irrep	Hadron	Irrep
π	A_{1u}^-	K	A_{1u}	η, η'	A_{1u}^+
ρ	T_{1u}^+	ω, ϕ	T_{1u}^-	K^*	T_{1u}
a_0	A_{1g}^+	f_0	A_{1g}^+	h_1	T_{1g}^-
b_1	T_{1g}^+	K_1	T_{1g}	π_1	T_{1u}^-
N, Σ	G_{1g}	Λ, Ξ	G_{1g}	Δ, Ω	H_g

Ensembles and run parameters

- plan to use three Monte Carlo ensembles
 - $(32^3|240)$: 412 configs $32^3 \times 256$, $m_\pi \approx 240$ MeV, $m_\pi L \sim 4.4$
 - $(24^3|240)$: 584 configs $24^3 \times 128$, $m_\pi \approx 240$ MeV, $m_\pi L \sim 3.3$
 - $(24^3|390)$: 551 configs $24^3 \times 128$, $m_\pi \approx 390$ MeV, $m_\pi L \sim 5.7$
- anisotropic improved gluon action, clover quarks (stout links)
- QCD coupling $\beta = 1.5$ such that $a_s \sim 0.12$ fm, $a_t \sim 0.035$ fm
- strange quark mass $m_s = -0.0743$ nearly physical (using kaon)
- work in $m_u = m_d$ limit so $SU(2)$ isospin exact
- generated using RHMC, configs separated by 20 trajectories

- stout-link smearing in operators $\xi = 0.10$ and $n_\xi = 10$
- LapH smearing cutoff $\sigma_s^2 = 0.33$ such that
 - $N_v = 112$ for 24^3 lattices
 - $N_v = 264$ for 32^3 lattices
- source times:
 - 4 widely-separated t_0 values on 24^3
 - 8 t_0 values used on 32^3 lattice

Excited states from correlation matrices

- in finite volume, energies are discrete (neglect wrap-around)

$$C_{ij}(t) = \sum_n Z_i^{(n)} Z_j^{(n)*} e^{-E_n t}, \quad Z_j^{(n)} = \langle 0 | O_j | n \rangle$$

- not practical to do fits using above form
- define new correlation matrix $\tilde{C}(t)$ using a single rotation

$$\tilde{C}(t) = U^\dagger C(\tau_0)^{-1/2} C(t) C(\tau_0)^{-1/2} U$$

- columns of U are eigenvectors of $C(\tau_0)^{-1/2} C(\tau_D) C(\tau_0)^{-1/2}$
- choose τ_0 and τ_D large enough so $\tilde{C}(t)$ diagonal for $t > \tau_D$
- effective energies

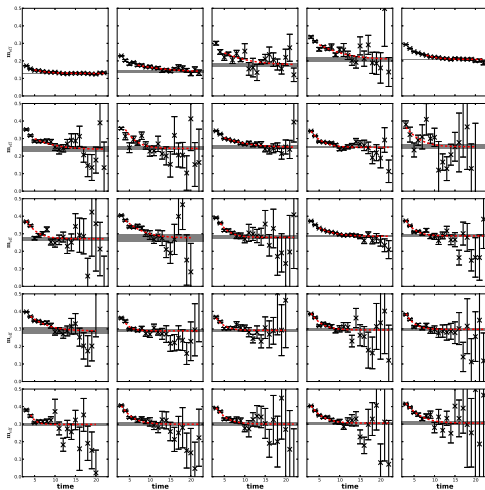
$$\tilde{m}_\alpha^{\text{eff}}(t) = \frac{1}{\Delta t} \ln \left(\frac{\tilde{C}_{\alpha\alpha}(t)}{\tilde{C}_{\alpha\alpha}(t + \Delta t)} \right)$$

tend to N lowest-lying stationary state energies in a channel

- 2-exponential fits to $\tilde{C}_{\alpha\alpha}(t)$ yield energies E_α and overlaps $Z_j^{(n)}$

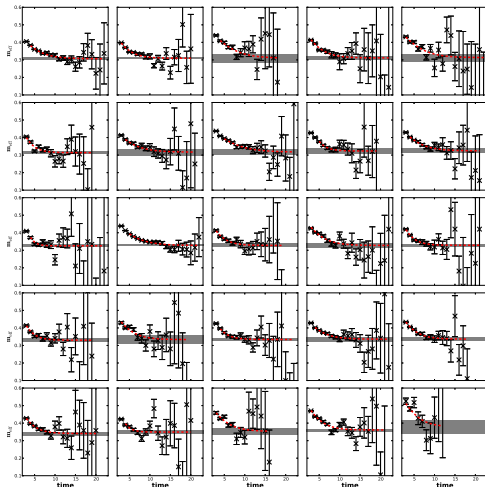
$I = 1, S = 0, T_{1u}^+$ channel

- effective energies $\tilde{m}^{\text{eff}}(t)$ for levels 0 to 24
- energies obtained from two-exponential fits



$I = 1, S = 0, T_{1u}^+$ energy extraction, continued

- effective energies $\tilde{m}^{\text{eff}}(t)$ for levels 25 to 49
- energies obtained from two-exponential fits

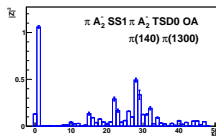
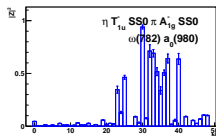
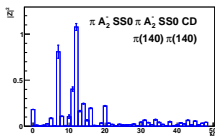
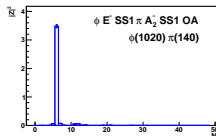
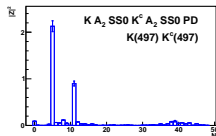
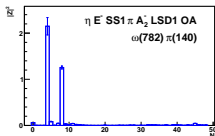
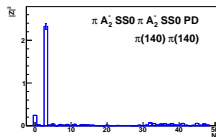
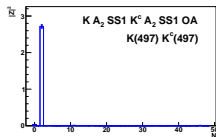
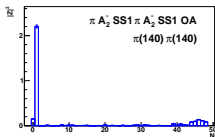


Level identification

- level identification inferred from Z overlaps with **probe** operators
- analogous to experiment: infer resonances from scattering cross sections
- keep in mind:
 - **probe** operators \bar{O}_j act on vacuum, create a “**probe state**” $|\Phi_j\rangle$,
 Z 's are overlaps of probe state with each eigenstate
 - have limited control of “probe states” produced by probe operators
$$|\Phi_j\rangle \equiv \bar{O}_j|0\rangle, \quad Z_j^{(n)} = \langle\Phi_j|n\rangle$$
 - ideal to be ρ , single $\pi\pi$, and so on
 - use of small- a expansions to characterize probe operators
 - use of smeared quark, gluon fields
 - field renormalizations
 - mixing is prevalent
 - identify by dominant probe state(s) whenever possible

Level identification

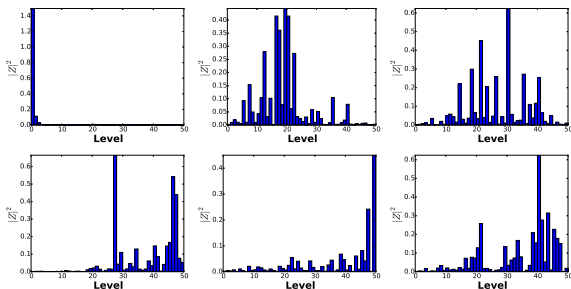
- overlaps for various operators



Identifying quark-antiquark resonances

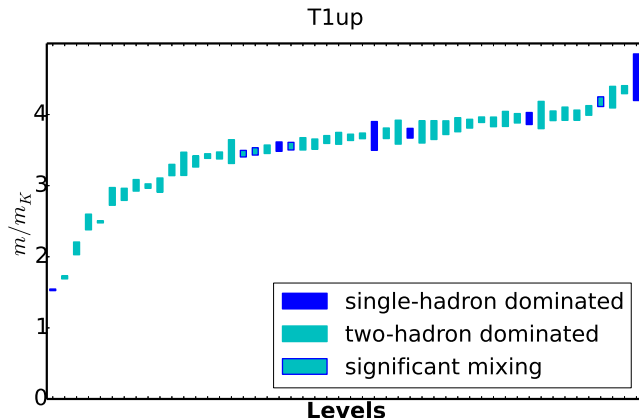
- resonances: finite-volume “precursor states”
- probes: *optimized* single-hadron operators
 - analyze matrix of just single-hadron operators $O_i^{[SH]}$ (12×12)
 - perform single-rotation as before to build probe operators
$$O'_m{}^{[SH]} = \sum_i v_i^{(m)*} O_i^{[SH]}$$
- obtain Z' factors of these probe operators

$$Z'_m{}^{(n)} = \langle 0 | O'_m{}^{[SH]} | n \rangle$$



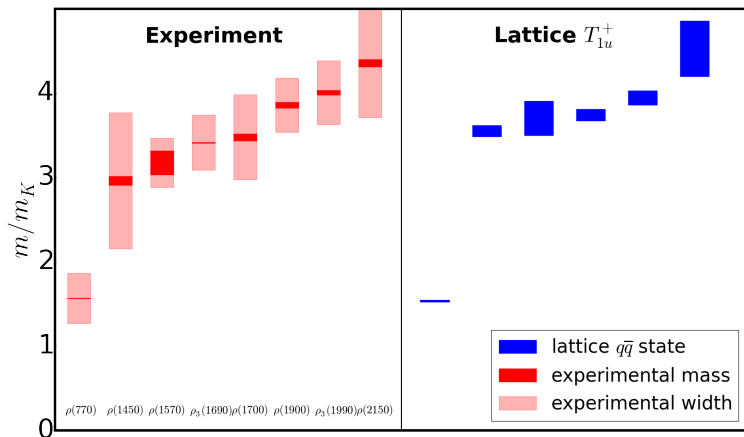
Staircase of energy levels

- stationary state energies $I = 1$, $S = 0$, T_{1u}^+ channel on $(32^3 \times 256)$ anisotropic lattice



Summary and comparison with experiment

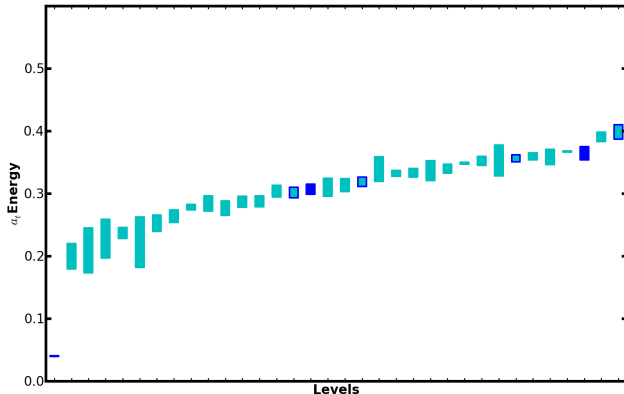
- right: energies of $\bar{q}q$ -dominant states as ratios over m_K for $(32^3|240)$ ensemble (resonance precursor states)
- left: experiment



Bosonic $I = 1, S = 0, A_{1u}^-$ channel

- finite-volume stationary-state energies: “staircase” plot
- $32^3 \times 256$ lattice for $m_\pi \sim 240$ MeV
- use of single- and two-meson operators only
- blue: levels of max overlaps with SH optimized operators

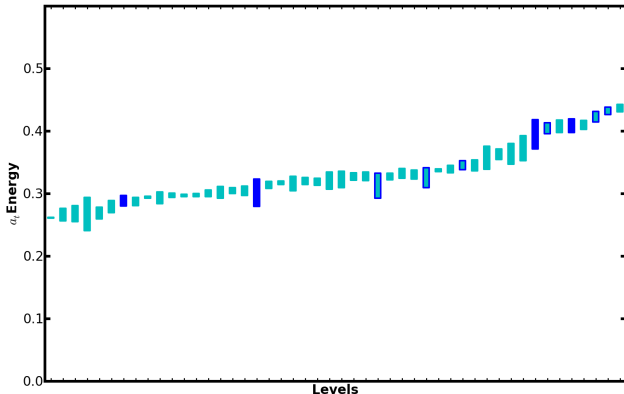
A1um 1



Bosonic $I = 1, S = 0, E_u^+$ channel

- finite-volume stationary-state energies: “staircase” plot
- $32^3 \times 256$ lattice for $m_\pi \sim 240$ MeV
- use of single- and two-meson operators only
- blue: levels of max overlaps with SH optimized operators

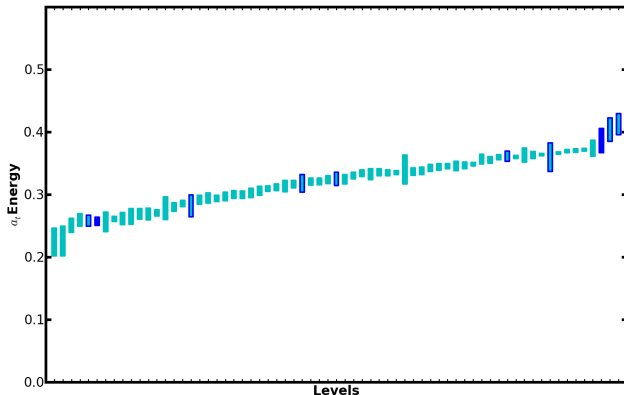
Eup 1



Bosonic $I = 1, S = 0, T_{1g}^-$ channel

- finite-volume stationary-state energies: “staircase” plot
- $32^3 \times 256$ lattice for $m_\pi \sim 240$ MeV
- use of single- and two-meson operators only
- blue: levels of max overlaps with SH optimized operators

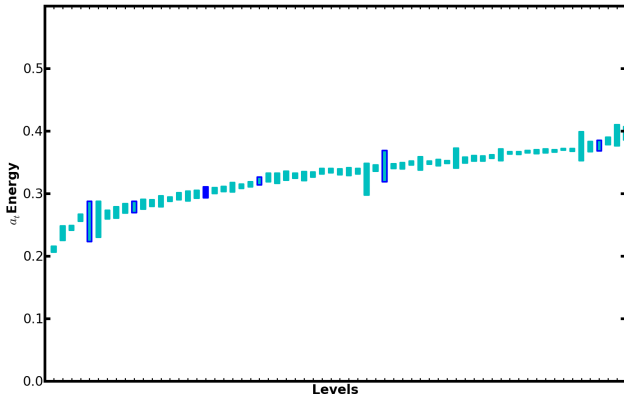
T1gm 1



Bosonic $I = 1, S = 0, T_{1u}^-$ channel

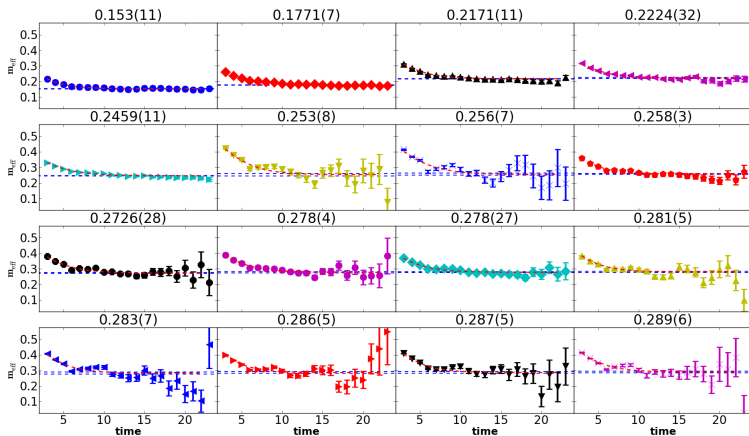
- finite-volume stationary-state energies: “staircase” plot
- $32^3 \times 256$ lattice for $m_\pi \sim 240$ MeV
- use of single- and two-meson operators only
- blue: levels of max overlaps with SH optimized operators

T1um 1



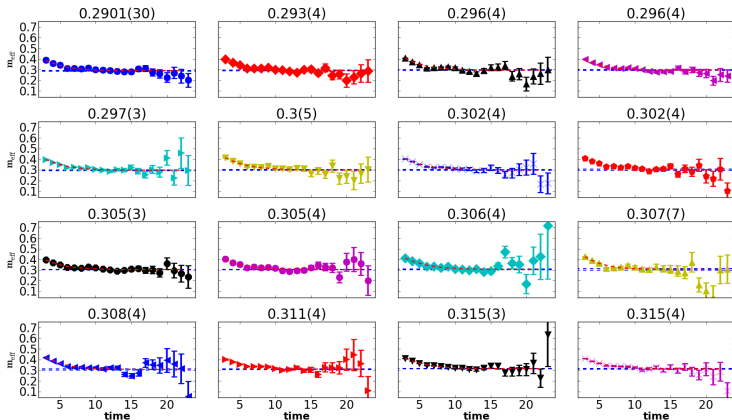
Bosonic $I = \frac{1}{2}$, $S = 1$, T_{1u} channel

- kaon channel: effective energies $\tilde{m}^{\text{eff}}(t)$ for levels 0 to 8
- results for $32^3 \times 256$ lattice for $m_\pi \sim 240$ MeV
- two-exponential fits



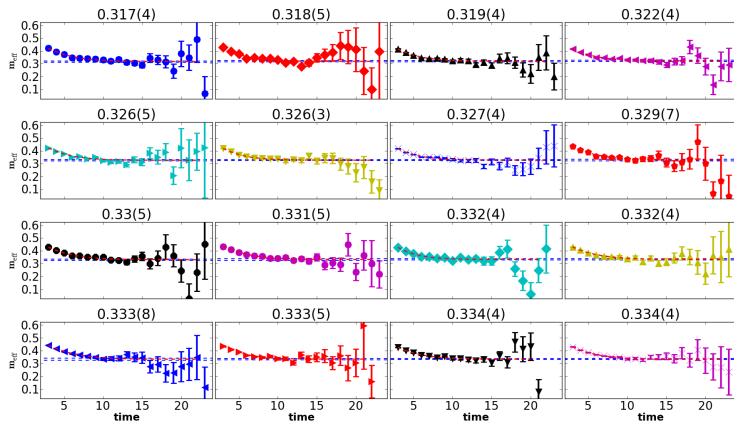
Bosonic $I = \frac{1}{2}$, $S = 1$, T_{1u} channel

- effective energies $\tilde{m}^{\text{eff}}(t)$ for levels 9 to 17
- results for $32^3 \times 256$ lattice for $m_\pi \sim 240$ MeV
- two-exponential fits



Bosonic $I = \frac{1}{2}$, $S = 1$, T_{1u} channel

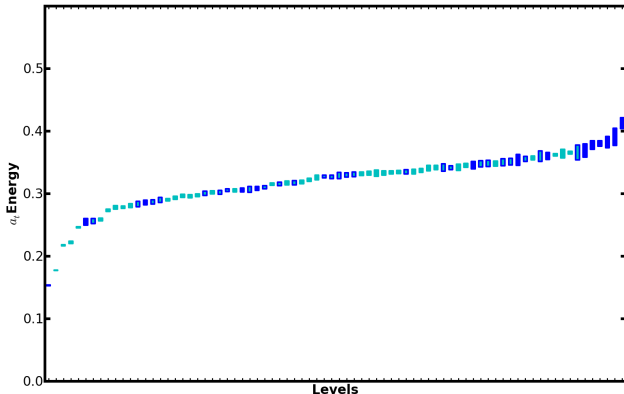
- effective energies $\tilde{m}^{\text{eff}}(t)$ for levels 18 to 23
- dashed lines show energies from single exponential fits



Bosonic $I = \frac{1}{2}$, $S = 1$, T_{1u} channel

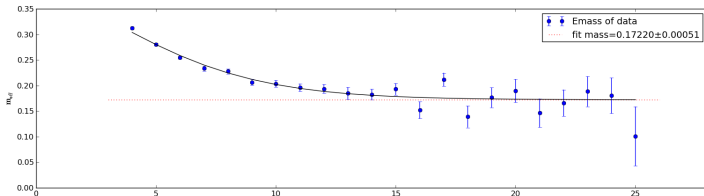
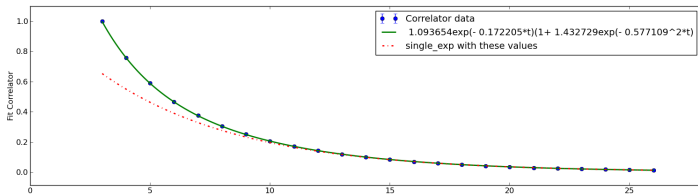
- finite-volume stationary-state energies: “staircase” plot
- $32^3 \times 256$ lattice for $m_\pi \sim 240$ MeV
- use of single- and two-meson operators only
- blue: levels of max overlaps with SH optimized operators

kaon T_{1u} 32



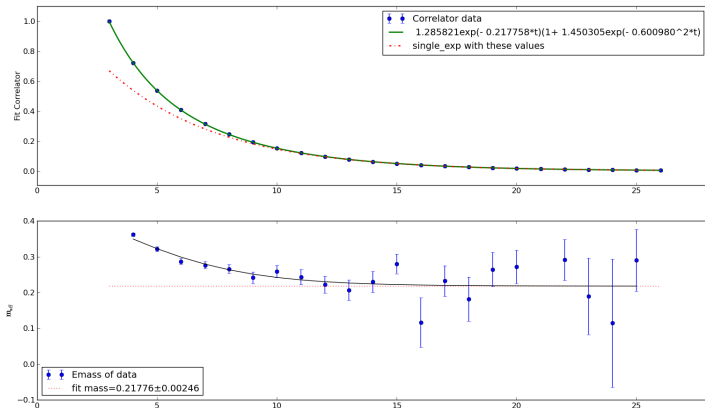
Preliminary $I = \frac{1}{2}$, $S = 1$, T_{1u} Results

- Lowest level diagonalized correlator fit
- $32^3 \times 256$ lattice for $m_\pi \sim 240$ MeV
- use of single- and two-meson operators only



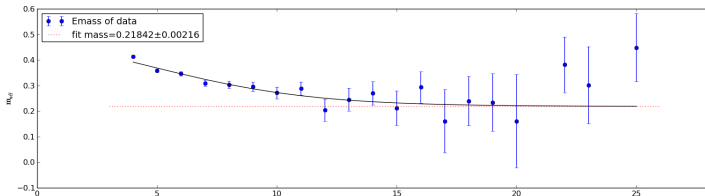
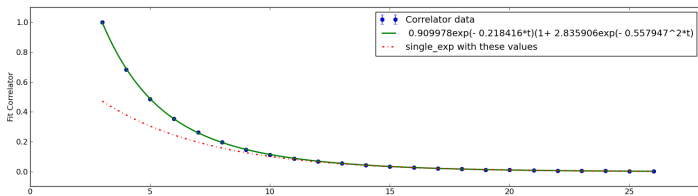
Preliminary $I = \frac{1}{2}$, $S = 1$, T_{1u} Results

- Second level diagonalized correlator fit
- $32^3 \times 256$ lattice for $m_\pi \sim 240$ MeV
- use of single- and two-meson operators only



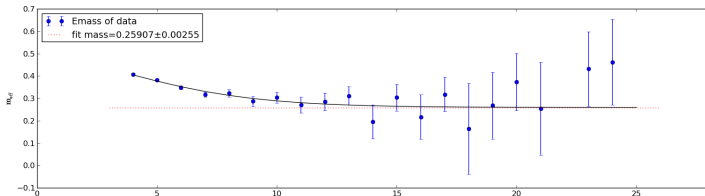
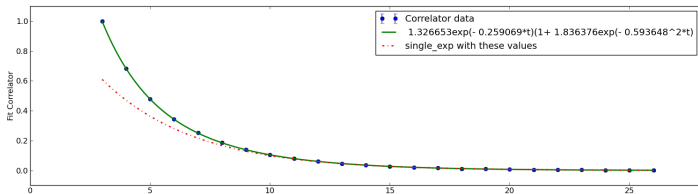
Preliminary $I = \frac{1}{2}$, $S = 1$, T_{1u} Results

- Third level diagonalized correlator fit
- $32^3 \times 256$ lattice for $m_\pi \sim 240$ MeV
- use of single- and two-meson operators only



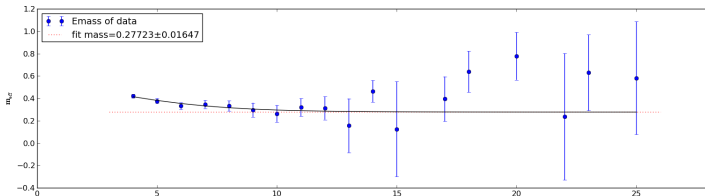
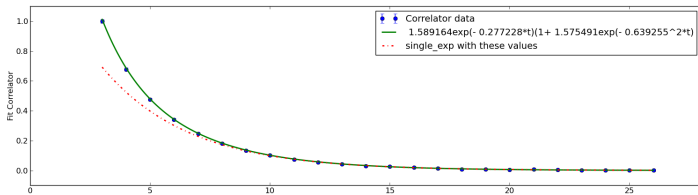
Preliminary $I = \frac{1}{2}$, $S = 1$, T_{1u} Results

- Fourth level diagonalized correlator fit
- $32^3 \times 256$ lattice for $m_\pi \sim 240$ MeV
- use of single- and two-meson operators only



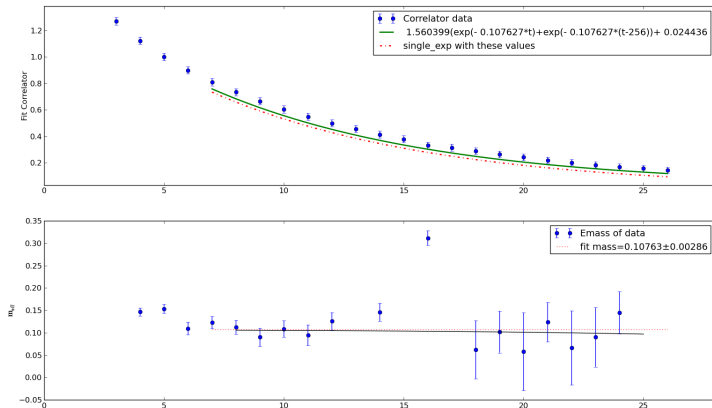
Preliminary $I = \frac{1}{2}$, $S = 1$, T_{1u} Results

- Fifth level diagonalized correlator fit
- $32^3 \times 256$ lattice for $m_\pi \sim 240$ MeV
- use of single- and two-meson operators only



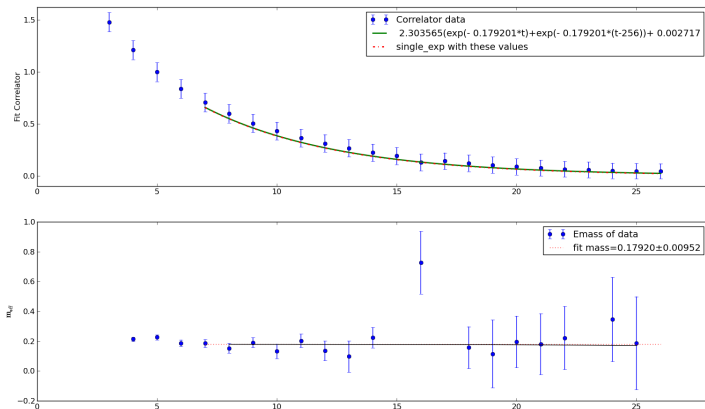
Preliminary $I = 0, S = 0, A_{1u}^+$ Results

- Lowest level diagonalized correlator fit
- $32^3 \times 256$ lattice for $m_\pi \sim 240$ MeV
- use of single-meson operators only



Preliminary $I = 0, S = 0, A_{1u}^+$ Results

- Second level diagonalized correlator fit
- $32^3 \times 256$ lattice for $m_\pi \sim 240$ MeV
- use of single-meson operators only



Scattering phase shifts from finite-volume energies

- correlator of two-particle operator σ in finite volume

$$C^L(P) = \text{diagram 1} + \text{diagram 2} + \text{diagram 3} + \dots$$

The diagram shows the expansion of the correlator $C^L(P)$ as a sum of terms. Each term consists of a sequence of circles connected by blue lines. The first circle is labeled σ and the last is labeled σ^\dagger . The intermediate circles are labeled iK . The first term has one iK circle. The second term has two iK circles. The third term has three iK circles. Dashed boxes enclose the iK circles in each term. Black dots are on top and blue dots are on bottom of the iK circles. The blue lines connect the dots between adjacent circles.

- Bethe-Salpeter kernel

$$iK = \text{diagram 1} + \text{diagram 2} + \text{diagram 3} + \text{diagram 4} + \text{diagram 5}$$

The diagram shows the decomposition of the Bethe-Salpeter kernel iK into five terms. The first term is a circle with two external lines. The second term is a crossing of two lines. The third term is a circle with two internal lines and two external lines. The fourth term is a circle with two internal lines and two external lines, with a different internal structure. The fifth term is a circle with two internal lines and two external lines, with a different internal structure. The sixth term is a circle with two internal lines and two external lines, with a different internal structure.

- $C^\infty(P)$ has branch cuts where two-particle thresholds begin
- momentum quantization in finite volume: cuts \rightarrow series of poles
- C^L poles: two-particle energy spectrum of finite volume theory

Phase shift from finite-volume energies (con't)

- finite-volume momentum sum is infinite-volume integral plus correction \mathcal{F}

The diagram shows an equality between three terms. On the left, a dashed box encloses two vertices: a black circle on top and a blue circle on bottom, connected by two arcs. This is equal to the sum of two terms. The first term is the same two-vertex structure without the dashed box. The second term is a vertical dashed line with a horizontal line crossing it, labeled with the symbol \mathcal{F} .

- define the following quantities: A , A' , invariant scattering amplitude $i\mathcal{M}$

The diagram shows three equations defining quantities as sums of diagrams:

- $A = \sigma + \sigma \circlearrowleft iK + \sigma \circlearrowleft iK \circlearrowleft iK + \dots$
- $A' = \sigma^\dagger + iK \circlearrowright \sigma^\dagger + iK \circlearrowright iK \circlearrowright \sigma^\dagger + \dots$
- $i\mathcal{M} = iK + iK \circlearrowleft iK + iK \circlearrowleft iK \circlearrowleft iK + \dots$

In these diagrams, σ and σ^\dagger are represented by circles with a horizontal line through them. iK is represented by a circle with a horizontal line through it. The arcs between circles are colored black or blue, and some contain a black dot.

Phase shifts from finite-volume energies (con't)

- subtracted correlator $C_{\text{sub}}(P) = C^L(P) - C^\infty(P)$ given by

$$C_{\text{sub}}(P) = \begin{array}{c} \textcircled{A} \text{---} \mathcal{F} \text{---} \textcircled{A'} + \textcircled{A} \text{---} \mathcal{F} \text{---} \textcircled{iM} \text{---} \mathcal{F} \text{---} \textcircled{A'} \\ + \textcircled{A} \text{---} \mathcal{F} \text{---} \textcircled{iM} \text{---} \mathcal{F} \text{---} \textcircled{iM} \text{---} \mathcal{F} \text{---} \textcircled{A'} + \dots \end{array}$$

- sum geometric series

$$C_{\text{sub}}(P) = A \mathcal{F} (1 - iM\mathcal{F})^{-1} A'.$$

- poles of $C_{\text{sub}}(P)$ are poles of $C^L(P)$ from $\det(1 - iM\mathcal{F}) = 0$

Phase shifts from finite-volume energies (con't)

- work in spatial L^3 volume with periodic b.c.
- total momentum $\mathbf{P} = (2\pi/L)\mathbf{d}$, where \mathbf{d} vector of integers
- masses m_1 and m_2 of particle 1 and 2
- calculate lab-frame energy E of two-particle interacting state in lattice QCD
- boost to center-of-mass frame by defining:

$$E_{\text{cm}} = \sqrt{E^2 - \mathbf{P}^2}, \quad \gamma = \frac{E}{E_{\text{cm}}},$$
$$\mathbf{q}_{\text{cm}}^2 = \frac{1}{4}E_{\text{cm}}^2 - \frac{1}{2}(m_1^2 + m_2^2) + \frac{(m_1^2 - m_2^2)^2}{4E_{\text{cm}}^2},$$
$$u^2 = \frac{L^2 \mathbf{q}_{\text{cm}}^2}{(2\pi)^2}, \quad \mathbf{s} = \left(1 + \frac{(m_1^2 - m_2^2)}{E_{\text{cm}}^2}\right) \mathbf{d}$$

- E related to S matrix (and phase shifts) by

$$\det[1 + F^{(\mathbf{s}, \gamma, u)}(S - 1)] = 0,$$

where F matrix defined next slide

Phase shifts from finite-volume energies (con't)

- F matrix in JLS basis states given by

$$F_{J'm_{J'}L'S'a'; Jm_JLSa}^{(\mathbf{s}, \gamma, u)} = \frac{\rho_a}{2} \delta_{a'a} \delta_{S'S} \left\{ \delta_{J'J} \delta_{m_{J'}m_J} \delta_{L'L} \right. \\ \left. + W_{L'm_{L'}; Lm_L}^{(\mathbf{s}, \gamma, u)} \langle J'm_{J'} | L'm_{L'}, Sm_S \rangle \langle Lm_L, Sm_S | Jm_J \rangle \right\},$$

- total angular mom J, J' , orbital mom L, L' , intrinsic spin S, S'
- a, a' channel labels
- $\rho_a = 1$ distinguishable particles, $\rho_a = \frac{1}{2}$ identical

$$W_{L'm_{L'}; Lm_L}^{(\mathbf{s}, \gamma, u)} = \frac{2i}{\pi \gamma u^{l+1}} \mathcal{Z}_{lm}(\mathbf{s}, \gamma, u^2) \int d^2\Omega Y_{L'm_{L'}}^*(\Omega) Y_{lm}^*(\Omega) Y_{Lm_L}(\Omega)$$

- Rummukainen-Gottlieb-Lüscher (RGL) shifted zeta functions \mathcal{Z}_{lm} defined next slide
- $F^{(\mathbf{s}, \gamma, u)}$ diagonal in channel space, mixes different J, J'
- recall S diagonal in angular momentum, but off-diagonal in channel space

RGL shifted zeta functions

- compute \mathcal{Z}_{lm} using

$$\begin{aligned}\mathcal{Z}_{lm}(\mathbf{s}, \gamma, u^2) &= \sum_{\mathbf{n} \in \mathbb{Z}^3} \frac{\mathcal{Y}_{lm}(\mathbf{z})}{(\mathbf{z}^2 - u^2)} e^{-\Lambda(\mathbf{z}^2 - u^2)} \\ &+ \delta_{l0} \gamma \pi e^{\Lambda u^2} \left(2u D(u\sqrt{\Lambda}) - \Lambda^{-1/2} \right) \\ &+ \frac{i^l \gamma}{\Lambda^{l+1/2}} \int_0^1 dt \left(\frac{\pi}{t} \right)^{l+3/2} e^{\Lambda t u^2} \sum_{\substack{\mathbf{n} \in \mathbb{Z}^3 \\ \mathbf{n} \neq 0}} e^{\pi i \mathbf{n} \cdot \mathbf{s}} \mathcal{Y}_{lm}(\mathbf{w}) e^{-\pi^2 \mathbf{w}^2 / (t\Lambda)}\end{aligned}$$

- where

$$\mathbf{z} = \mathbf{n} - \gamma^{-1} \left[\frac{1}{2} + (\gamma - 1) \mathbf{s}^{-2} \mathbf{n} \cdot \mathbf{s} \right] \mathbf{s},$$

$$\mathbf{w} = \mathbf{n} - (1 - \gamma) \mathbf{s}^{-2} \mathbf{s} \cdot \mathbf{n} \mathbf{s}, \quad \mathcal{Y}_{lm}(\mathbf{x}) = |\mathbf{x}|^l Y_{lm}(\hat{\mathbf{x}})$$

$$D(x) = e^{-x^2} \int_0^x dt e^{t^2} \quad (\text{Dawson function})$$

- choose $\Lambda \approx 1$ for convergence of the summation
- integral done Gauss-Legendre quadrature, Dawson with Rybicki

P -wave $I = 1$ $\pi\pi$ scattering

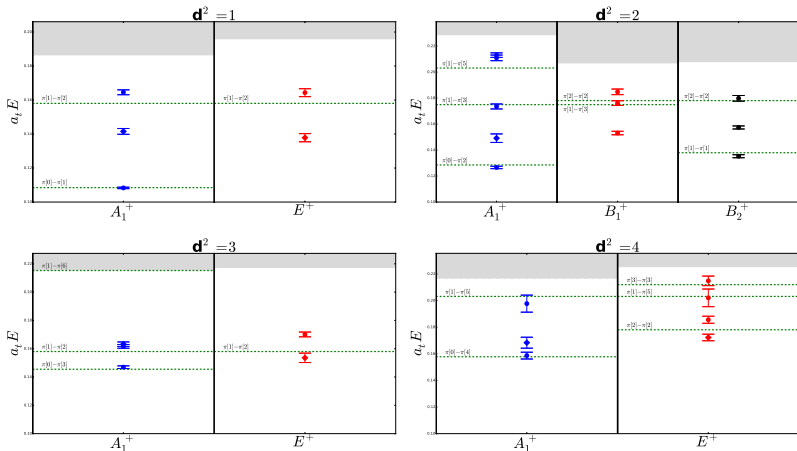
- for P -wave phase shift $\delta_1(E_{\text{cm}})$ for $\pi\pi$ $I = 1$ scattering
- define

$$w_{lm} = \frac{Z_{lm}(s, \gamma, u^2)}{\gamma \pi^{3/2} u^{l+1}}$$

d	Λ	$\cot \delta_1$
(0,0,0)	T_{1u}^+	$\text{Re } w_{0,0}$
(0,0,1)	A_1^+	$\text{Re } w_{0,0} + \frac{2}{\sqrt{5}} \text{Re } w_{2,0}$
	E^+	$\text{Re } w_{0,0} - \frac{1}{\sqrt{5}} \text{Re } w_{2,0}$
(0,1,1)	A_1^+	$\text{Re } w_{0,0} + \frac{1}{2\sqrt{5}} \text{Re } w_{2,0} - \sqrt{\frac{6}{5}} \text{Im } w_{2,1} - \sqrt{\frac{3}{10}} \text{Re } w_{2,2},$
	B_1^+	$\text{Re } w_{0,0} - \frac{1}{\sqrt{5}} \text{Re } w_{2,0} + \sqrt{\frac{6}{5}} \text{Re } w_{2,2},$
	B_2^+	$\text{Re } w_{0,0} + \frac{1}{2\sqrt{5}} \text{Re } w_{2,0} + \sqrt{\frac{6}{5}} \text{Im } w_{2,1} - \sqrt{\frac{3}{10}} \text{Re } w_{2,2}$
(1,1,1)	A_1^+	$\text{Re } w_{0,0} + 2\sqrt{\frac{6}{5}} \text{Im } w_{2,2}$
	E^+	$\text{Re } w_{0,0} - \sqrt{\frac{6}{5}} \text{Im } w_{2,2}$

Finite-volume $\pi\pi$ $I = 1$ energies

- $\pi\pi$ -state energies for various d^2
- dashed lines are non-interacting energies, shaded region above inelastic thresholds

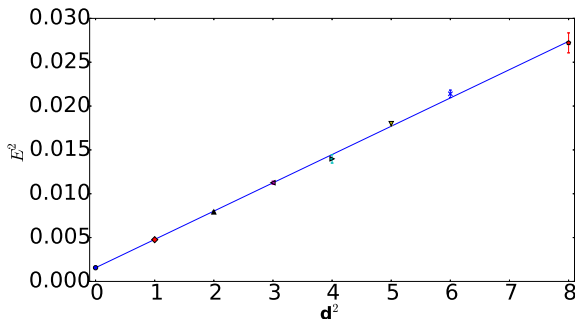


Pion dispersion relation

- boost to cm frame requires aspect ratio on anisotropic lattice
- aspect ratio ξ from pion dispersion

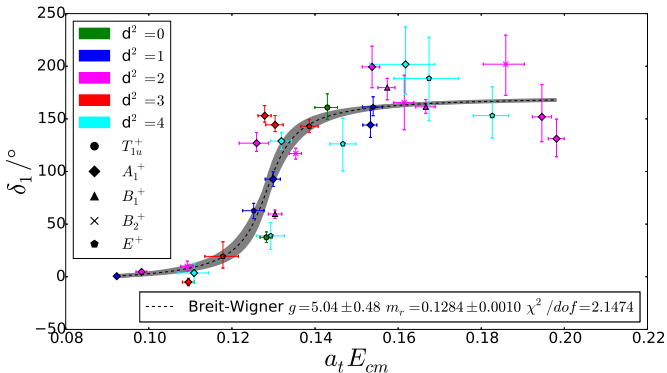
$$(a_t E)^2 = (a_t m)^2 + \frac{1}{\xi^2} \left(\frac{2\pi a_s}{L} \right)^2 \mathbf{d}^2$$

- slope below equals $(\pi/(16\xi))^2$, where $\xi = a_s/a_t$







$I = 1$ $\pi\pi$ scattering phase shift and width of the ρ

- preliminary results $32^3 \times 256$, $m_\pi \approx 240$ MeV
- additional collaborator: Ben Hoerz (Dublin)



- fit $\tan(\delta_1) = \frac{\Gamma/2}{m_r - E} + A$ and $\Gamma = \frac{g^2}{48\pi m_r^2} (m_r^2 - 4m_\pi^2)^{3/2}$

References

-  S. Basak et al., *Group-theoretical construction of extended baryon operators in lattice QCD*, Phys. Rev. D **72**, 094506 (2005).
-  S. Basak et al., *Lattice QCD determination of patterns of excited baryon states*, Phys. Rev. D **76**, 074504 (2007).
-  C. Morningstar et al., *Improved stochastic estimation of quark propagation with Laplacian Heaviside smearing in lattice QCD*, Phys. Rev. D **83**, 114505 (2011).
-  C. Morningstar et al., *Extended hadron and two-hadron operators of definite momentum for spectrum calculations in lattice QCD*, Phys. Rev. D **88**, 014511 (2013).

Conclusion

- goal: comprehensive survey of energy spectrum of QCD stationary states in a finite volume
- stochastic LapH method works very well
 - allows evaluation of all needed quark-line diagrams
 - source-sink factorization facilitates large number of operators
 - `last_laph` software completed for evaluating correlators
- analysis software `sigmond` urgently being developed
- analysis of 20 channels $I = 1, S = 0$ for $(24^3|390)$ and $(32^3|240)$ ensembles nearing completion
- can evaluate and analyze correlator matrices of unprecedented size 100×100 due to XSEDE resources
- study various scattering phase shifts also planned
- infinite-volume resonance parameters from finite-volume energies \rightarrow need new effective field theory techniques